JOURNAL OF MATERIALS SCIENCE 15 (1980) 82–88

Morphology of thermal etch-pits formed on GaP surfaces

MASAHIRO KITADA
Central Research Laboratory, Hitachi Ltd, Kokubunji, Tokyo 185, Japan

The morphology of thermal etch-pits in GaP single crystal surface induced by heating in a low vacuum is investigated. On heating at 950° C, tetrahedral etch-pits with four (1 1 0) facets are formed on the (1 1 0) plane. Etch-pits with (1 0 0), (1 1 0), and (1 1 1) facets are formed at 1000° C, and tetrahedral pits with radiating groove-like pits develop above 1050° C. Trigonal pits with (1 1 0) walls and (1 1 1) bottom are formed on the $(1\,1\,1)_B$ plane, and hexagonal pits with (1 1 1) and (1 2 1) walls and (0 1 1) bottom are formed on the (1 1 0) cleavage surface. The etch-pit density is about $10^6\ cm^{-2}$ and is independent of heating temperature. The apparent activation energy for etch-pit growth is about 2.2 eV. It is established that dislocation is one of the primary sources of etch-pit formation.

1. Introduction
Thermal etch-pits are known to be formed by local sublimation of atoms from crystal surfaces. Several studies of thermal etch-pit formation in III–V compounds have been reported [1–3]. The pits of these compounds have been shown to form according to the dissociation reaction

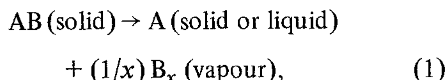

$$AB\,(\text{solid}) \rightarrow A\,(\text{solid or liquid}) + (1/x)\,B_x\,(\text{vapour}), \qquad (1)$$

where $x = 1, 2$, or 4 in most cases [3], and A and B are IIIB and VB Group elements, respectively. Thus when the above reaction occurs locally on a crystal surface, etch-pits are formed. The growth of such pits is known to be promoted by impurity atoms existing in the furnace atmosphere as well as in the crystal surface [4].

In GaAsP light emitting diode, thermal etch-pits can destroy p–n junctions [5], and in GaP surfaces, they have sometimes been observed during semiconductor device preparation [6]. The appearance of such pits can be due to both residual gas and dopant impurities in the heat-treatment system. The etch-pit growth rate is also influenced by the heat-treatment temperature [1].

This work examines the temperature dependence of the thermal etch-pit morphology of GaP in a comparatively low vacuum, as well as the growth rate of such pits.

2. Experimental procedure
The studies in the present work were carried out on (1 0 0) and $(1\,1\,1)_B$ epitaxy faces, and the (1 1 0) cleavage face of an epitaxy crystal using both electron microscope and microbalance techniques. These techniques yield the etch-pit morphology and the absolute vaporization rate by monitoring the weight loss of a single crystal specimen with known area as a function of time.

The materials used were sulphur-doped single crystal GaP having a donor concentration of 3 to $5 \times 10^{17}\ cm^{-3}$, a nitrogen concentration of 1 to $3 \times 10^{19}\ cm^{-3}$, and a dislocation density of about $5 \times 10^4\ cm^{-2}$. The vapour-phase epitaxial (1 0 0), liquid phase epitaxial $(1\,1\,1)_B$, and cloven (1 1 0) specimen were slightly etched by HCl–HNO_3 in a ratio of 2 : 1. They were rinsed sufficiently in de-ionized water before heat treatment.

The specimens were placed in a clean, dry quartz tube and heated at 800 to 1100° C for 15 min in a vacuum of 5×10^{-4} Torr. In the microbalance experiment, the crystal surfaces were locally covered by a vapour-deposited SiO_2 film to define the vaporization area.

Vapour emitted from the crystal surface was detected by a mass-spectrometer.

0022–2461/80/010082–07\$02.70/0 © *1980 Chapman and Hall Ltd.*

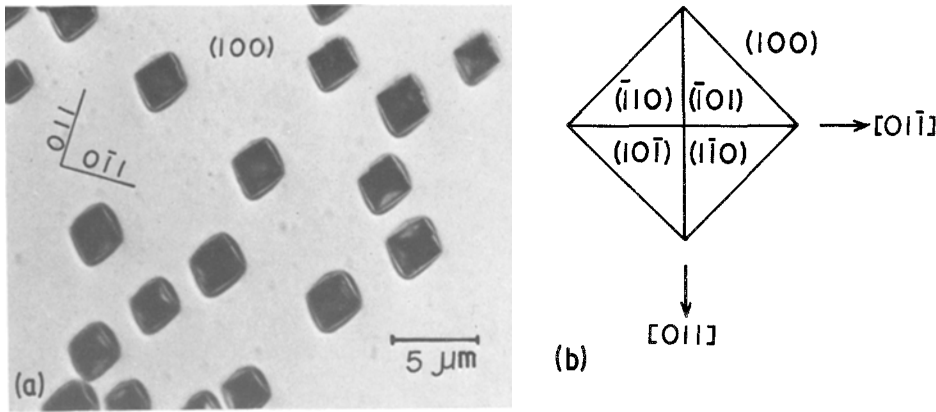

Figure 1 (a) Thermal etch-pits on GaP (1 0 0) surface treated at 900° C and (b) facets.

3. Results

3.1. Morphology of thermal etch-pits

3.1.1. (1 0 0) surface

On the GaP (1 0 0) surface, thermal etch-pits with clear facets were observed above 900° C in a vacuum of 5×10^{-4} Torr. Typical thermal etch-pits on the (1 0 0) surface are shown in Fig. 1a. These pits have four equivalent (1 1 0) facets as drawn in Fig. 1b.

As the temperature was raised from 900 to 1000° C, more complex etch-pits were observed. Thermal etch-pits formed at 1000° C are shown in Fig. 2a. The (1 1 0) facets of these pits have many steps and (1 1 1) facets appeared at the corners of the pits. A magnified electron micrograph of a pit corner is given in Fig. 2b. Small steps were also observed on the (1 1 0) facet as indicated by arrows in Fig. 2b. Tilting analysis with an electron microscope showed the crystal plane of these steps to be near (1 0 0).

A transmission electron micrograph of small pits on a (1 0 0) surface treated at 1050° C for 3 min is shown in Fig. 3. These pits had (1 0 0) and (1 1 1) facets, and (1 0 0) bottom.

An optical micrograph of the thermal etch-pits on the (1 0 0) surface treated at 1050° C for 15 min is shown in Fig. 4a. Many radiating pits can be observed around the main pit. A scanning electron micrograph of a pit having radiating pits is shown in Fig. 4b. The main pit had four (1 1 0) and eight (1 1 1) facets and a (1 0 0) bottom as drawn in Fig. 5. These radiating

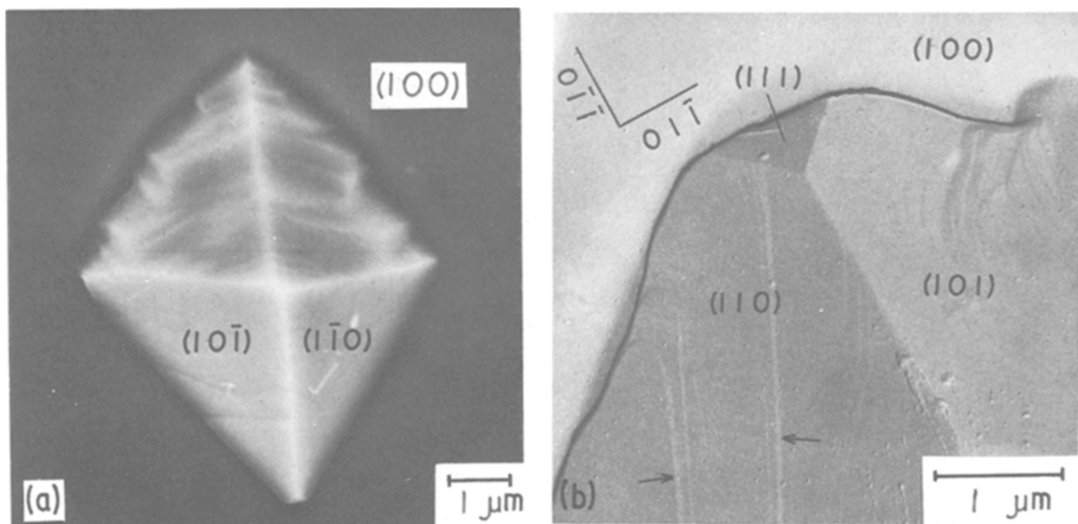

Figure 2 Electron micrographs of thermal etch-pit on GaP (1 0 0) surface treated at 1000° C. (a) SEM image, (b) magnification of pit corner.

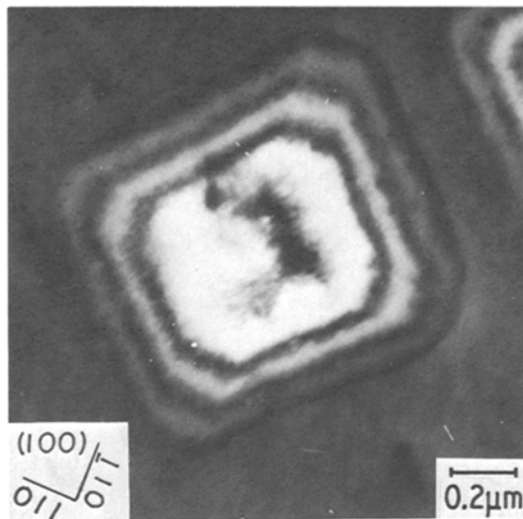

Figure 3 Transmission electron micrograph of thermal etch-pit on GaP (1 0 0) surface treated at 1050° C for 3 min.

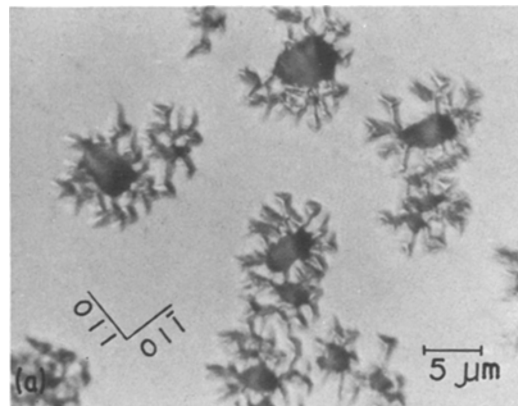

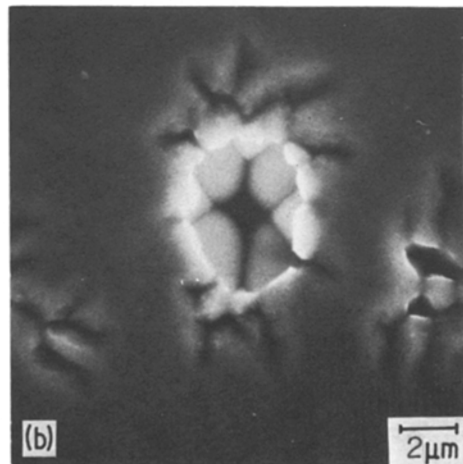

Figure 4 Thermal etch-pit with radiating pits on GaP (1 0 0) surface treated at 1050° C for 15 min. (a) Optical micrograph, (b) SEM image.

pits formed along [1 1 0]. A transmission electron micrograph of groove-like pits that formed along the dislocation lines is shown in Fig. 6a, and the pits formed at the crossing position between the dislocation line and the crystal surface are shown in Fig. 6b. This shows that the pits originate at the dislocation lines.

The pits on the (1 0 0) GaP surface treated at 850° C for 2 h are shown in Fig. 7. Pits with clean facets were not observed. This is because such pits are very shallow, and thermal evaporation sufficient to form pits with clean facets does not occur. Thermal etch-pits did not appear below 850° C. The temperature and treating time dependencies of the shape of thermal etch-pit formed on the (1 0 0) GaP surface are shown in Fig. 8. The facets are the (1 1 0) type in the low-temperature range, becoming more complex at high temperature. Pit size increased with temperature and treatment time.

3.1.2. (1 1 0) surface

Typical etch-pits formed on the (1 1 0) GaP surface after treating at 1050° C for 15 min are shown in Fig. 9a. The shape shown in Fig. 9b was also observed, but very rarely. The facets of a typical pit determined by the SEM tilting technique are indicated in Fig. 10. The facets of the pit wall are (1 1 1) and (1 1 2), and the bottom is (1 0 1). In the complex-shaped pit, the development of the (1 0 0) normal to the (1 1 0) crystal plane is as

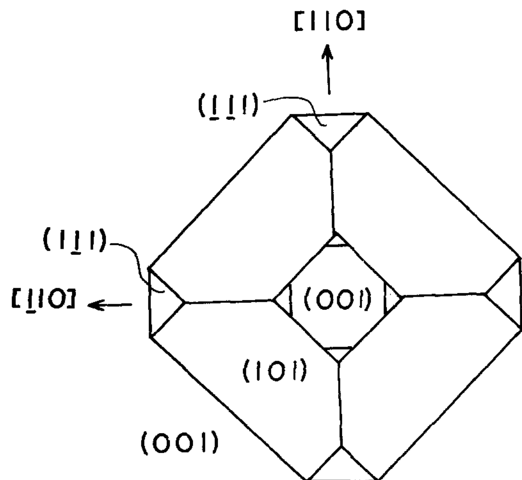

Figure 5 Schematic representation of the facets of thermal etch-pit on GaP (1 0 0) surface treated at 1050° C for 15 min.

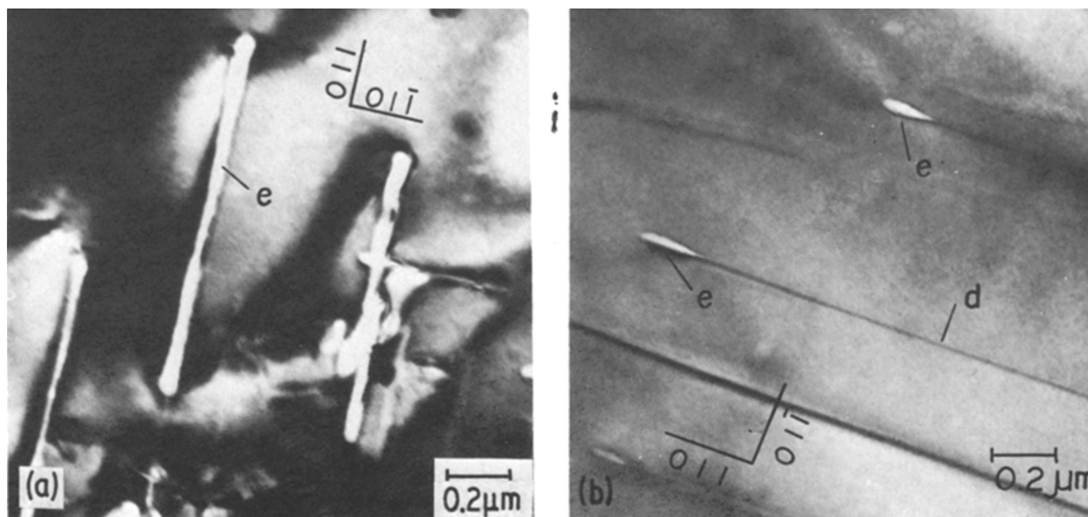

Figure 6 Electron micrographs of (a) groove-like pits that formed along dislocation lines and (b) etch-pits that formed at cross points between dislocation lines and surface.

indicated by the arrow in Fig. 9b. The pit density was greatest around steps formed by a cleavage of the crystal. A row of pits along the cleavage step is shown in Fig. 11.

3.1.3. $(1\,1\,1)_B$ surface

Typical thermal etch-pits formed on the $(1\,1\,1)_B$ GaP surface are shown in Fig. 12a. The pits had a flat triangular bottom and the walls were (1 1 0) while the bottom was $(1\,1\,1)_B$. The pits developed planarly. Therefore, it is estimated that the etching rate for (1 1 0) is larger than that for $(1\,1\,1)_B$. The facets of the pit are indicated in Fig. 12b.

3.2. Etch-pit density

The etch-pit densities measured are shown in Fig. 13. The densities on the (1 0 0), (1 1 0), and $(1\,1\,1)_B$ specimens were 3 to 5 x 10^6, 3 to 8 x 10^6, and 5 to 9 x 10^6 cm^{-2}, respectively, and no temperature dependence was observed. The densities depend on neither the crystal plane nor treating time.

3.3. Vaporization rate and vapour analysis

The vaporization rate of a specimen with a (1 0 0) surface is shown in Fig. 14. The relation between the vaporization rate and the reciprocal tempera-

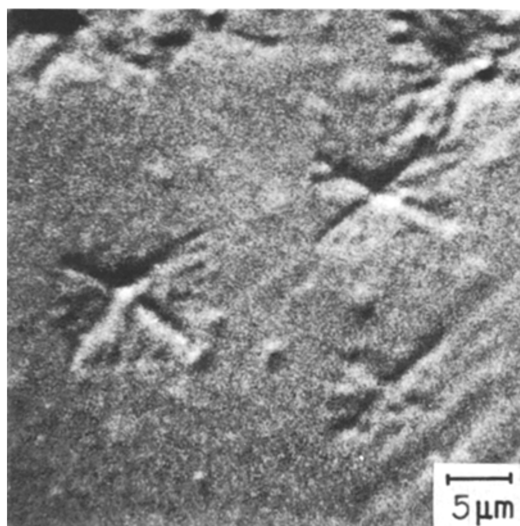

Figure 7 SEM image of thermal etch-pits on GaP (1 0 0) surface treated at 850° C for 2 h.

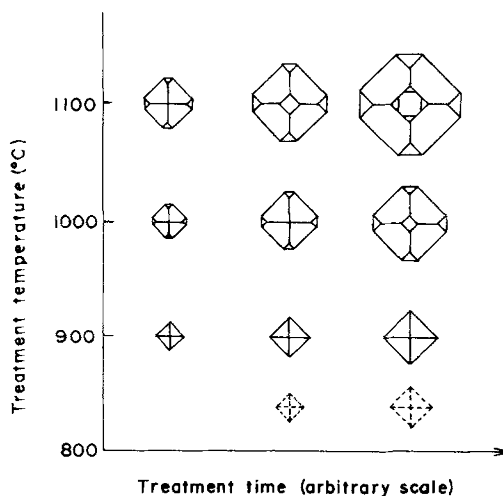

Figure 8 Temperature and treating time dependencies of the shape of thermal etch-pits formed on the (1 0 0) GaP surface.

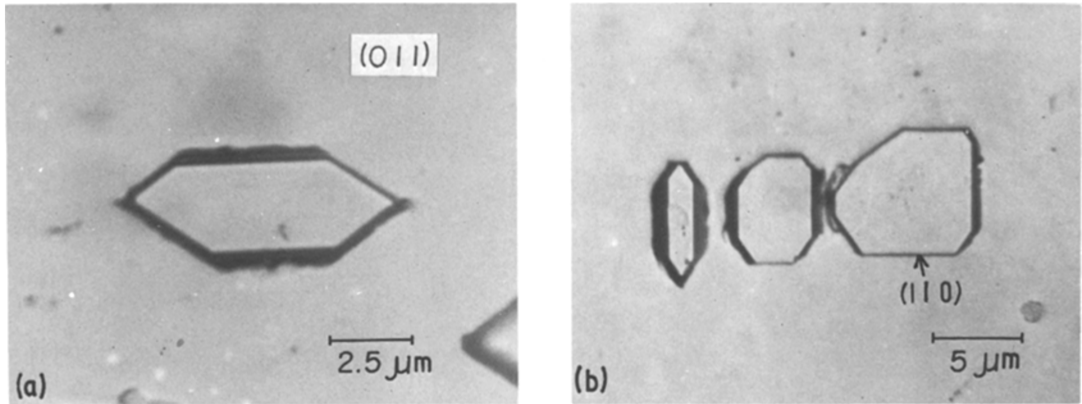

Figure 9 (a) Typical thermal etch-pits on GaP (1 1 0) surface treated at 1050° C for 15 min, and (b) complex etch-pit.

ture is linear. The apparent activation energy of vaporization (or etch-pit formation) is about 2.2 eV. In the vapour emitted from the crystal surface, PO_3 and GaO were detected by mass-spectrometry.

4. Discussion

From the study of the epitaxial growth of diamond-type crystals, Blizanakov and Delineschev [7] reported the following theoretical equilibrium faces of the crystal: (1 1 1), (1 0 0), (1 1 0), (3 1 1), and (3 1 0). For example, Simov [8] observed (1 0 0), (1 1 1), and (1 1 0) faces in CdS growth by evaporation. It is fundamentally expected that the thermal etch-pit formation is the reverse phenomenon of such crystal growth. The equilibrium faces of the thermal etch-pit, therefore, should be similar to the equilibrium faces appearing when crystals grow. However, the degree of equilibrium is dependent on the interatomic force between the first neighbours. Fischer and Heasell [2] observed triangular pits on the $(1\,1\,1)_B$ surface and rectangular pits on the (1 0 0) surface of InSb, but the facets were not determined. Lou and Somorjai [1] also reported triangular pits on the GaAs (1 1 1) surface. These pits intersected each other and formed terraced macroscopic ledges, but the types of facets were not reported. As mentioned above, it is possible that (1 1 1), (1 0 0), (1 1 0), (3 1 1), and (3 1 0) facets appear. In this work, (1 0 0), (1 1 0), (1 1 1), and (1 1 2) facets were observed, but (3 1 1) and (3 1 0) facets could not be recognized.

In normal vaporization under high vacuum, the elements of III–V compounds vaporize dissociatively according to the reaction [1]

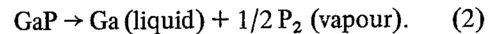

$$GaP \rightarrow Ga\,(\text{liquid}) + 1/2\,P_2\,(\text{vapour}). \quad (2)$$

However, in a low vacuum containing many O_2 and H_2O molecules as in this experiment, it is assumed that the compound reacts selectively with oxygen and water in the atmosphere and that the pits are formed by the following reactions:

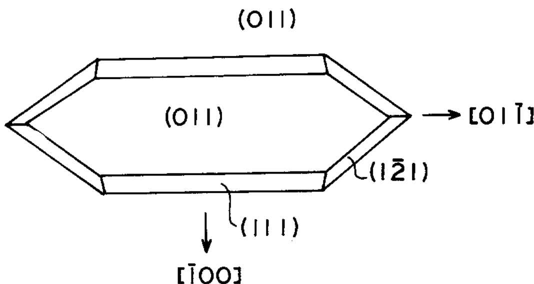

Figure 10 Schematic representation of facets of typical thermal etch-pit formed on GaP (1 1 0) surface.

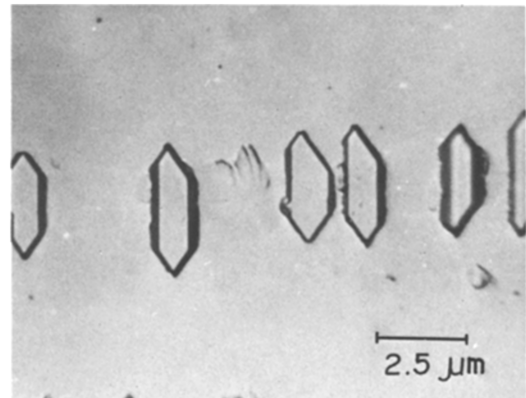

Figure 11 Row of thermal etch-pits along cleavage step on GaP (1 1 0) cleavage surface.

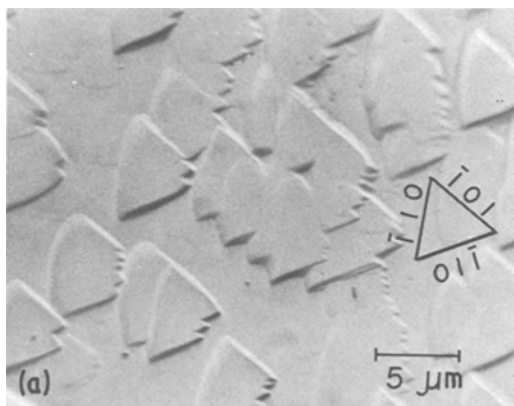

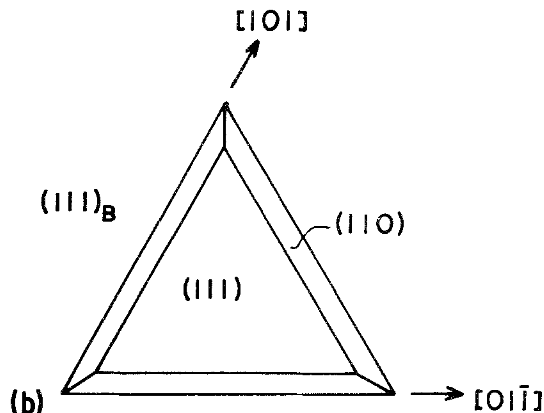

Figure 12 (a) Typical thermal etch-pits formed on GaP $(1\,1\,1)_B$ surface, and (b) facets.

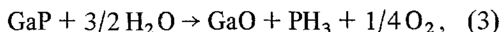

$$GaP + 3/2\,H_2O \rightarrow GaO + PH_3 + 1/4\,O_2, \quad (3)$$

$$4GaP + 7O_2 \rightarrow 4GaO + 2P_2O_5. \quad (4)$$

Since PO_3 and GaO were detected by mass spectrometry and liquid Ga was not observed on the specimen surface, it is considered that the pits were formed by one or both of the above reactions, even though P_2O_5 was not detected. In addition, the apparent activation energy obtained indicates the activation process of the above reactions. The activation energy relating to GaAs vaporization which obeys reaction 1 is 3.3 to 3.9 eV [1]. The activation energy 2.2 eV obtained in this work is smaller than that of GaAs. Therefore, in a low vacuum, it is assumed that vaporization of the compound is promoted by the existing O_2 and H_2O.

The lattice structure around dislocations is severely distorted over several adjacent unit cells, and the atomic bond just under the dislocation line is broken. Since this area is very sensitive to physical (normal vaporization), and chemical reactions to impurities, the stress surrounding the dislocation is sufficient to make this the favoured site for pit nucleation [9]. Etch-pit formation in the area surrounding the dislocation was observed in this experiment as shown in Figs. 4 and 6. However, the dislocation density measured is about $5 \times 10^4\,cm^{-2}$. If the dislocations do not move during etching, flat-bottom pits are not observed. Therefore, it is thought that other surface defects also become activation points. These may be kinks, steps, and impurity atoms on the crystal surface. Since the etch-pit density around cleavage steps was larger than that in the no-step region as shown in Fig. 11, it seems clear that the steps are one of the activation points. Fischer and Heasell [2] observed a similar development of the etch-pit along a grain boundary on the InSb (1 0 0) surface. In general, when surface

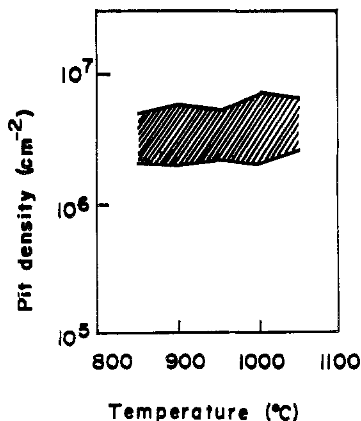

Figure 13 Densities of thermal etch-pits formed on GaP surface treated at various temperatures in 5×10^{-4} Torr.

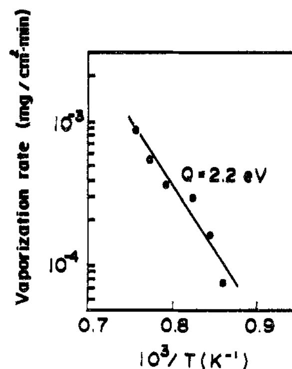

Figure 14 Vaporization rate as a function of reciprocal temperature for thermal etch-pit formation on GaP (1 0 0) surface.

impurities are present, they enhance pit formation. Since impurities stick to the steps easily, enhancement by impurities is also a possibility.

On the other hand, the groove-like radiating pits around the main pit, as shown in Fig. 4, are thought to be related to the dislocation lines induced during main pit formation. The multiplication of dislocations from the origin is assumed to be due to stress by the etch-pit formation.

The (1 0 0) surface was removed preferentially from the crystal surface. The rates of removal decrease in the order (1 1 0), (1 1 1), and (1 0 0). These differences are considered to be attributable to rate differences of the above reactions. The vaporization process is very complex and involves the following reaction steps; bulk diffusion, charge transfer, bond breaking, dissociation of the vaporizing surface atoms [10]. It also involves chemical reactions with impurities on the crystal surface and in the atmosphere. The chemical reaction is dominant in this experiment as mentioned above, but the rate limiting steps for vaporization could not be determined from the results of this work. Therefore, further studies would be necessary to clarify the rate differences of vaporization in future.

The temperature dependence of the pit morphology is also considered to be due to the temperature dependence of the reactivity difference betwene the crystal faces.

References

1. C. Y. LOU and G. A. SOMORJAI, *J. Appl. Phys.* **55** (1971) 4554.
2. C. FISCHER and E. HEASELL, *Surface Sci.* **30** (1972) 592.
3. P. GOLDFINGER, in "Compound Semiconductors", Vol. 1, edited by R. K. Willardson (Reinhold, New York, 1962).
4. R. C. SCHOONMAKER, A. BUHL and J. LEMLEY, *J. Phys. Chem.* **69** (1965) 3455.
5. H. SATOH and M. KITADA, Proceedings of Spring Meeting, (Japanese Applied Physics Society, 1976) p. 29a-m-9.
6. M. KITADA, unpublished work.
7. G. BLIZNAKOV and S. SELINESCHEV, *Phys. Stat. Sol.* **13** (1966) 101.
8. S. SIMOV, *Thin Solid Films* **15** (1973) 79.
9. H. C. GATOS and M. C. LAVINE, *J. Electrochem. Soc.* **107** (1960) 427.
10. J. G. DAVY, Ph.D. thesis, University of California, Berkeley (1970).

Received 13 March and accepted 6 June 1979.